Field Crops Research 231 (2019) 93–104

Contents lists available at ScienceDirect

Field Crops Research

journal homepage: www.elsevier.com/locate/fcr

Explicit wheat production model adjusted for semi-arid environments

Ofir Miller[a], David Helman[b,*,1], Tal Svoray[a,e], Efrat Morin[c], David J. Bonfil[d]

[a] Department of Geography and Environmental Development, Ben-Gurion University of the Negev, Beer-Sheva, 8410501, Israel
[b] Department of Geography and the Environment, Bar-Ilan University, Ramat Gan, 5290002, Israel
[c] Institute of Earth Sciences, Hebrew University of Jerusalem, E. J. Safra Campus, Jerusalem, 9190401, Israel
[d] Department of Vegetable and Field Crop Research, Agricultural Research Organization, Gilat Research Center, 8531100, Israel
[e] Department of Psychology, Ben-Gurion University of the Negev, Beer-Sheva, 8410501, Israel

ARTICLE INFO

Keywords:
GIS
Grain yield
HYDRUS
Wheat
Climate change

ABSTRACT

Current literature suggests that wheat production models are limited either to wide-scale or plot-based predictions ignoring pattern of habitat conditions and surficial hydrological processes. We present here a high-spatial resolution (50 m) non-calibrated GIS-based wheat production model for predictions of aboveground wheat biomass (AGB) and grain yield (GY). The model is an integration of three sub-models, each simulating elemental processes relevant for wheat growth dynamics in water-limited environments: (1) HYDRUS-1D, a finite element model that simulates one-dimensional movement of water in the soil profile; (2) a two-dimensional GIS-based surface runoff model; and (3) a one-dimensional process-driven mechanistic wheat growth model. By integrating the three sub-models, we aimed to achieve a more accurate spatially continuous water balance simulation with a better representation of root zone soil water content (SWC) impacts on plant development. High-resolution grid-based rainfall data from a meteorological radar system were used as input to HYDRUS-1D. Twenty-two commercial wheat fields in Israel were used to validate the model in two seasons (2010/11 and 2011/12). Results show that root zone SWC was accurately simulated by HYDRUS-1D in both seasons, particularly at the top 10-cm soil layer. Observed vs simulated AGB and GY were highly correlated with R^2 = 0.93 and 0.72 (RMSE = 171 g m^{-2} and 70 g m^{-2}) having low biases of -41 g m^{-2} (8%) and 52 g m^{-2} (10%), respectively. Model sensitivity test showed that HYDRUS-1D was mainly driven by spatial variability in the input soil characteristics while the integrated wheat production model was mostly affected by rainfall spatial variability indicating the importance of using accurate high-resolution rainfall data as model input. Using the integrated model, we predict decreases in AGB and GY of *c.* 10.5% and *c.* 12%, respectively, for 1 °C of warming and *c.* 7.7% and *c.* 7.3% for 5% reduction in rainfall amount in our study sites. The suggested model could be used by scientists to better understand the causes of spatial and temporal variability in wheat production and the consequences of future scenarios such as climate change.

1. Introduction

Crop models are increasingly being used in agriculture to support decision-making and planning at a large spatial scale, particularly in relation to risks associated to climate change issues such as decreases in yield and/or soil fertility (Rosenzweig et al., 2014; Schauberger et al., 2017; Wu et al., 2016). Among these models, process-based crop growth simulation models are the most useful in predicting crop responses to climate because they attempt to explain the mechanism of the processes rather than simply provide parameter predictions such as statistical models and models based on empirical relationships do (Challinor et al., 2009; Chenu et al., 2017; Holzkämper, 2017). Crop growth models have been originally developed at the plot scale and more recently used and evaluated at the regional and global scale but with a rather coarse spatial resolution. These models have been used to study the impacts of projected climate change over large agricultural areas (Challinor et al., 2016; Deryng et al., 2014; Zhao et al., 2017) but need to be adjusted for smallholding farm applications.

Process-based crop models are used to simulate crop growth dynamics and yield predictions under diverse management practices, climate and environmental conditions (Chenu et al., 2017). These models are either driven by plot-based meteorological information acquired from weather stations providing estimates at the plot scale (e.g. Brisson et al., 2003; Stöckle et al., 2003), or by grid-based modelled

* Corresponding author.
E-mail address: david.helman@biu.ac.il (D. Helman).
[1] Currently at the Department of Earth and Planetary Sciences, Johns Hopkins University, Baltimore, MD, USA.

https://doi.org/10.1016/j.fcr.2018.11.011
Received 10 July 2018; Received in revised form 6 November 2018; Accepted 15 November 2018
Available online 28 November 2018
0378-4290/

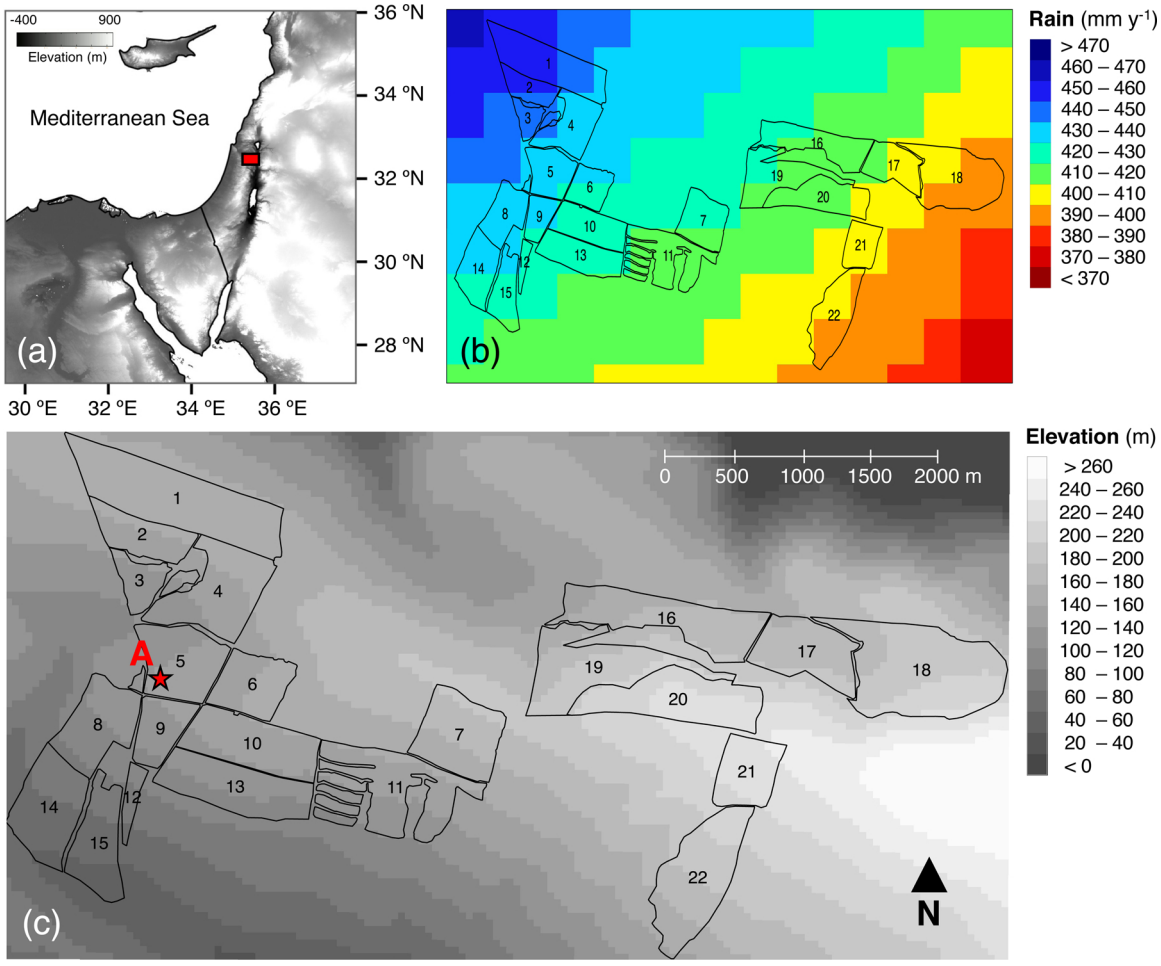

Fig. 1. (a) Location of the study area at Ramot Yssakhar, Northern Israel, and **(b–c)** the 22 wheat fields used in this study to test and validate the model. **(b)** The northwest to southeast mean annual rainfall gradient (20-year average) in the study area (Israel Meteorological Service) and **(c)** topographic elevation are shown. Elevation was extracted from the 50-m DEM layer, which was also used as a basis for the spatial resolution of the model. Red star in **(c)** indicates the general location (A) in which the 12 Decagon 10HS sensors for the SWC measurements were placed (For interpretation of the references to colour in this figure legend, the reader is referred to the web version of this article).

climate data, providing estimates at a regional to global scale but at a very coarse spatial resolution (at least a few to hundreds of kilometers, e.g. Stöckle et al., 2014). Due to a lack of spatial continuity in input weather data and/or the too coarse spatial resolution of climate data, these models suffer from a poor representation of water dynamics at the root zone essential to feedback process-based mechanistic crop models. The lack of a proper surface physics simulation, such as SWC dynamics, may result in model uncertainties, particularly in crops growing under water-limited conditions (Helman et al., 2019; Rajala et al., 2009).

To provide a better application to local conditions model predictions are often downscaled using either statistical or dynamic downscaling approaches (Fowler et al., 2007). However, such downscaling efforts might introduce biases in terms of unaccounted specific temperature extremes or rainfall patterns that could bias the simulated growth dynamics and yield (Cammarano et al., 2013; Cammarano and Tian, 2018; Hansen and Jones, 2000). Moreover, downscaled results may involve a high degree of uncertainty related to the original model parameters and model structure (Palosuo et al., 2011).

To overcome these drawbacks, the use of a one-dimensional mechanistic crop model is suggested for local applications (Boogaard et al., 1998; Brisson et al., 2009). The one-dimensional mechanistic model uses meteorological information acquired from a near weather station as an input instead of using a grid-based modelled climate data, providing estimates at the field/farm level. These kinds of models have been successfully applied in the estimation of wheat, maize and rice yields providing a potential decision supporting tool for local farming (Attia et al., 2016; Corbeels et al., 2016; Lopez et al., 2017).

Though promising, it requires the use of many input variables, which are often unavailable or difficult to acquire. It also lacks the spatially continuous representation needed to cope with issues of spatial variability in local soils and other environmental characteristics, which have been shown to affect crop yield production (Jégo et al., 2015). A combination of approaches is therefore suggested for merging process-based models using GIS tools to simulate crop growth processes over large areas with a relatively high spatial resolution (Huffman et al., 2015; Liu, 2009; Thorp et al., 2008).

A Digital Elevation Model (DEM) layer, for example, may provide high-resolution grid-based information relevant for computing topographic models (Tarboton, 1997) and potential incident radiation load (Fu and Rich, 2002), necessary for a more accurate simulation of plant growth in the one-dimensional mechanistic crop model (Amir and Sinclair, 1991a, 1991b). Meteorological radars may provide a more accurate grid-based rainfall data than statistical interpolation between weather stations, particularly in areas where rainfall is highly variable in time and space (Marra and Morin, 2015; Morin and Gabella, 2007).

Integrating the grid-based information with a simple mechanistic plant growth model in a geographic information system (GIS) environment may provide a spatially continuous estimation of crop production and yield at a very high spatial resolution (of a few tens of meters). Moreover, the high-resolution spatial hydrologic information

may be used as an input into a one-dimensional hydrological model to improve SWC dynamics simulations providing a more accurate information on the available SWC at the root zone, which makes it an important factor in crop development and productivity (Lawes et al., 2009), particularly in water-limited environments (Acevedo et al., 1999; Amir and Sinclair, 1991b; Helman et al., 2018).

Here, we combine a one-dimensional Richard's equation-based hydrological model with a two-dimensional runoff model and a mechanistic wheat growth model (Amir and Sinclair, 1991b, 1991a) on a grid-based GIS platform to provide high resolution aboveground wheat biomass and grain yield estimates. The integrated model, linking different processes on a grid-based platform, may be important for estimating AGB and GY variations in our region that present variable topography and significant slopes. To assess the importance of our integrated approach we first tested the spatial and temporal accuracy of the integrated model in 22 commercial wheat fields in Israel, validating the model with in-situ SWC, AGB and GY measurements (Section 3.1). Then, we examined the spatial sensitivity of the models through fixing each input parameter per model run (Section 3.2). Finally, we used the model to simulate field-level AGB and GY variations expected from projected rainfall and temperature changes in our region (Section 3.3).

2. Materials and methods

2.1. Study area

The model was used in the study area located at Ramot Yssakhar (32°35′38.76″N, 35°27′48.96″E; Fig. 1a), which is a relatively hilly region in Northern Israel. At Ramot Yssakhar, there are numerous crop fields with a total agricultural area of *c.* 30 km^2. Elevation in Ramot Yssakhar ranges between -150 and *c.* 270 m above sea level (m.a.s.l.) with a more narrow range of 30 and 260 m.a.s.l. at the area of the 22 fields used in this study (Fig. 1c). Typical slopes are 1° to 30°, with an average slope for the study area of 5°. Soils are mostly brown basaltic grumusols with a high content of clays (50%–66%), which were developed on local basaltic rocks. The mean annual rainfall amount in the study area is 430 mm y^{-1} with a noted gradient of high to low rainfall amounts from north-western to the south-eastern fields (Fig. 1b and Goldreich, 1994). Rainfall is concentrated in an average of 61 days out of the six month comprising the rainy season period (November – April), with mean daily rainfall amount < 10 mm d^{-1}.

Fig. 1b,c show the 22 wheat fields that were used to test HYDRUS-1D and the integrated wheat growth model in seasons 2010/11 and 2011/2012. Wheat (*Triticum aestivum* L.) varieties were grown in 18 out of the 22 fields in 2010/11 and in only 13 out of the 22 fields in 2011/12 (Table 1).

Table 1 summarizes the characteristics of the 22 fields in terms of soil hydraulic parameters, cultivar, sowing date and land use management (LUM) practiced in the two seasons.

2.2. Field measurements and validation

An average of three soil samples per field (i.e. 3 × 22 samples) was collected to derive for each field the five soil hydraulic parameters required for HYDRUS-1D: saturated and residual soil water contents - θ_s and θ_r (both in $m^3 m^{-3}$); two parameters in the soil water retention function - α (in m^{-1}) and n (unitless); and the saturated hydraulic conductivity - K_s (in mm h^{-1}). For each soil sample, soil composition and soil grain size were determined using the hydrometer method (Gee and Bauder, 1979) and averaged per field. The average composition of the soils was then used to derive the five hydraulic parameters per field from Rosetta (Van Genuchten, 1980; Table 1), which is a computer program that estimates soil hydraulic parameters from soil composition and other soil characteristics through a series of hierarchical pedotransfer functions.

In order to validate HYDRUS-1D and the integrated wheat model, volumetric SWC, AGB and end-of-season GY were measured for each of the two seasons (2010/11 and 2011/12). SWC was estimated at the top 5–10 cm and at a deeper 30-cm depth in two ways: (1) gravimetrically, by drying at 105 °C for 24 h a set of four soil samples, which were collected from 40 randomly selected 50-m cells (a total of 4 × 40 samples) and converting the weighted water content into volumetric SWC by multiplying by the sample's bulk density; (2) by using Decagon 10HS sensors placed at the abovementioned depths (5–10 cm and 30-cm) in 12 randomly distributed plots within a single 50-m cell (Location A; red star in Fig. 1c), which was randomly selected from a set of cells that were found to be the most representative of the average characteristics of the soils in the studied area (i.e. average over all fields). Gravimetric measurements were conducted approximately every week while Decagon 10HS sensors recorded SWC every 10 min, from December to April of 2010/11 and 2011/2012 seasons.

AGB was collected from the same 40 randomly selected cells used to derive the gravimetric SWC, with an average of four AGB samples collected per cell at different stages of the wheat growth period: three times during 2010/11 (23-Jan, 15-Feb and 8-May) and twice in 2011/12 (29-Nov and 6-Feb). Information on GY was acquired from the farmers per field at the end of the growing seasons from 13 fields in 2010/11 and 7 fields in 2011/12.

2.3. GIS database

A 50-m grid cell DEM layer (Israel Mapping Center) was used as a basis for the spatial resolution of the input/output layers in/from the wheat production model (Fig. 1c). The DEM layer was used to produce three different input layers used in the surface runoff model: (1) a grid-based flow-direction layer, which was produced following the procedure proposed by Takken et al. (2001); (2) a flow accumulation grid-based layer, which is the accumulated weighted amount of water flowing into each downslope cell in the raster layer from of neighboring cells. This last layer was produced from (1) using the Flow Accumulation ArcGIS tool (Jenson and Domingue, 1988); and (3) a 50-m raster layer of daily incoming solar radiation factor (f_{Rg}; unitless) produced from the DEM and the Hemispherical Viewshed algorithm ArcGIS tool (Fu and Rich, 2002). Measured R_g from the nearest meteorological station (< 7 km southwest to the study area) was used to calibrate the f_{Rg} layer to get actual daily R_g values (in MJ m^{-2} d^{-1}). Daily incident photosynthetic active radiation (PAR) was then calculated as 45.7% from the actual R_g (Nagaraja Rao, 1984).

Rainfall data were acquired from the C-band radar system of Shacham Mekorot located at Ben-Gurion airport (31.989169 N, 34.9021917E). Raw radar reflectivity data (Z, $mm^6 m^{-3}$) obtained at 5-min time resolution and at 1.4° x 1 km spatial resolution (equivalent to about 2 km^2 over the study site) were converted to rain intensity (R, mm h^{-1}) using a power-law relationship, $Z = 316R^{1.5}$, and a mean bias adjustment on a daily basis using a near-by rain gauge (< 5 km south to the study site) (Morin and Gabella, 2007). Radar rainfall estimates were validated through the use of the mean bias adjustment method (see V8 and Table 3 in Morin and Gabella, 2007). For a close by region, the storm-weighted mean fractional standard error from the radar was found to be 47%, which is considered adequate estimation from radars. Gauge interpolation, for example, produced larger errors of > 60% for the same case. Data were further interpolated to 1-min and 50-m resolution to match HYDRUS-1D model requirements.

Agro-technical information that includes: seeding date, cultivar, cultivar's maturity classification type (i.e. early, moderate or late) and LUM practice (i.e. CT – conventional tillage; NT – no tillage; and NTS – no tillage covered with straw) was collected per field from the farmers in both seasons (Table 1).

All data were adjusted to the spatial resolution of the models, which was based on the 50-m DEM layer. A short description of all input parameters and their specific functions in the integrated wheat production model may be found in Table S1 in *Appendix A*.

Table 1
Summary of field characteristics (Field# is the same as in Fig. 1) and land use management practiced during the two studied seasons of 2010/11 and 2011/12.

	Soil hydraulic parameters					2010/11				2011/12			
Field #	θ_s	θ_r	α	n	K_s	Cultivar	Maturity	Sowing	LUM	Cultivar	Maturity	Sowing	LUM
1	0.545	0.107	0.020	1.278	22.135	Ged	medium	26/11/10	NTS	–	–	–	–
2	0.545	0.107	0.019	1.289	22.690	Ged	medium	23/11/10	CT	Gal	late	24/11/11	NTS
3	0.545	0.107	0.020	1.285	22.770	Ged	medium	23/11/10	CT	Gal	late	24/11/11	NTS
4	0.546	0.107	0.020	1.283	22.055	Ged/Bar/BtS	medium	22/11/10	CT	Ged	medium	06/12/11	NTS
5	0.547	0.109	0.021	1.255	20.830	Ged	medium	10/12/10	NT	Ged	medium	07/12/11	NTS
6	0.547	0.109	0.021	1.255	20.830	Ged	medium	28/11/10	CT	–	–	–	–
7	0.542	0.106	0.019	1.292	23.953	Yuv	early	29/11/10	CT	Ged	medium	04/12/11	CT
8	0.545	0.107	0.020	1.275	22.430	Galil	late	05/12/10	NT	Ged	medium	14/11/11	CT
9	0.545	0.107	0.020	1.285	22.770	Ged	medium	10/11/10	NT	Ged	medium	13/11/11	CT
10	0.550	0.109	0.021	1.260	18.750	BtS	medium	24/11/10	CT	–	–	–	–
11	0.536	0.104	0.019	1.309	26.068	BtS	medium	22/11/10	NT	BtS	medium	23/11/11	NT
12	0.542	0.109	0.019	1.292	23.953	–	–	–	–	Ged	medium	08/12/11	NT
13	0.550	0.109	0.021	1.260	18.750	–	–	–	–	Ged	medium	04/12/11	CT
14	0.531	0.103	0.019	1.317	28.200	–	–	–	–	Ged	medium	13/11/11	CT
15	0.546	0.107	0.020	1.281	21.690	Ged	medium	10/11/10	CT	Gal	late	13/11/11	NT
16	0.547	0.108	0.020	1.278	21.127	Neg	late	30/11/10	CT	–	–	–	–
17	0.547	0.108	0.020	1.278	21.127	Ged	medium	08/11/10	CT	–	–	–	–
18	0.547	0.108	0.020	1.278	21.127	Ged	medium	10/11/10	NT	–	–	–	–
19	0.547	0.108	0.020	1.278	21.127	–	–	–	–	Nir	late	04/12/11	NT
20	0.531	0.103	0.019	1.317	28.200	Nir	late	30/11/10	NT	–	–	–	–
21	0.571	0.107	0.019	1.289	20.530	Ged	medium	22/11/10	NT	–	–	–	–
22	0.542	0.107	0.020	1.284	24.010	Nir	late	22/11/10	CT	–	–	–	–

Soil hydraulic parameters: θ_s and θ_r – saturated and residual soil water contents, respectively; α and n – parameters in the soil water retention function; and K_s – the saturated hydraulic conductivity. Practiced land use management (LUM): CT – conventional tillage; NT – no tillage; and NTS – no tillage with straw cover. Cultivar: Ged – Gedera; Bar – Bar-Nir; BtS – Bet Ha'Shita; Yuv – Yuval; Neg – Negev; Nir – Nirit; Gal – Galil. Cultivar maturity classification (late, medium, early).

2.4. Model description

Fig. 2 presents the conceptual flowchart of the integrated model along its input, output and validation datasets. Input that is constant within a field is indicated in grey. HYDRUS-1D is driven by soil characteristics and meteorology while root growth is provided by the crop model. Water availability, as rainfall and lateral surface flow, derived from the weather radar and the spatially distributed runoff model is used as input for HYDRUS-1D.

The spatially distributed runoff model is driven by topography, agronomic characteristics of the field and excess of water derived from HYDRUS-1D. The crop model is driven by meteorology, agronomic characteristics and available water at the root zone profile (FTSW), which is provided by HYDRUS-1D.

2.4.1. The HYDRUS-1D model

The HYDRUS-1D is a public domain Windows-based modeling environment for analysis of water flow in saturated porous media (https://www.pc-progress.com/en/Default.aspx?hydrus-1d). The HYDRUS-1D model uses a Galerkin-type linear finite element solution to solve the one-dimensional Richards' equation with a time step integration achieved by implicit (backwards) finite difference scheme for both saturated and unsaturated conditions (Simunek et al., 2005). HYDRUS-1D may be used to analyze water and solute movement in

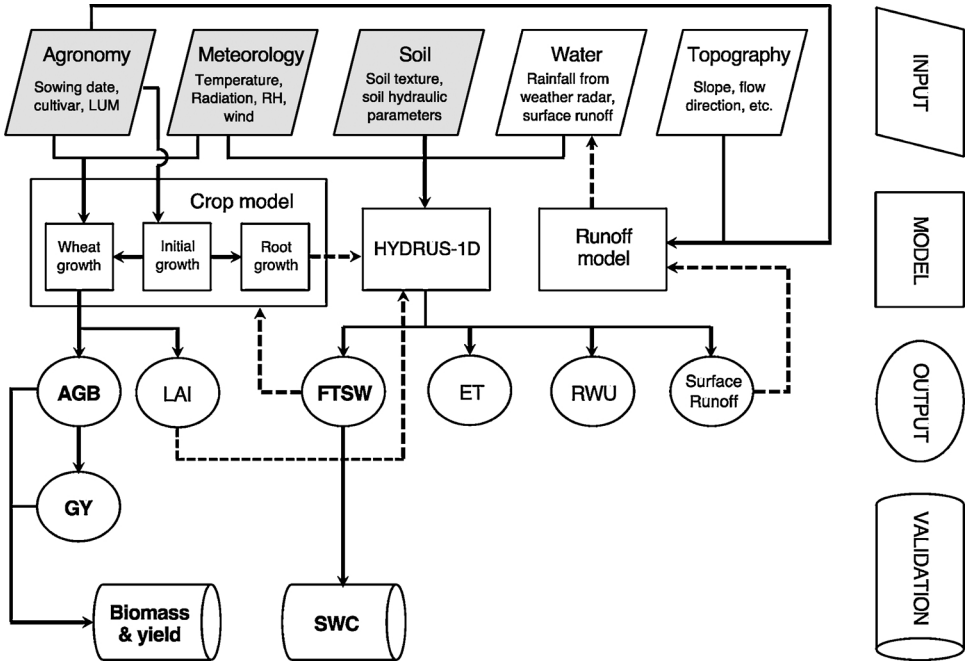

Fig. 2. Conceptual flowchart of the integrated wheat production model alongside its input, output and validation datasets. Constant input within a field is indicated in grey while variable input within a field is in white. All input variables where grid adjusted on GIS platform. Dashed arrows indicate feedback flows into the models. AGB and GY are aboveground biomass and grain yields, respectively (both in g m^{-2}); LAI is leaf area index ($m^2\,m^{-2}$); FTSW is the fraction of transpirable soil water at the root-zone (see text); ET is actual evapotranspiration (mm m^{-2}); and RWU is the root water uptake (mm m^{-2}).

unsaturated, partially saturated, or fully saturated porous media. The flow equation incorporates a sink term to account for water uptake by plant roots.

Because our integrated model accounts for a daily expansion of roots length a feedback flow from/to the wheat growth model is required (Fig. 2). HYDRUS^{-1}D has several hydrological outputs from which we used five in our integrated model:

(i) *Actual evapotranspiration* (*ET*), which is calculated in HYDRUS^{-1}D using Penman-Monteith potential *ET* (ET_0) equation limited by soil water content (Simunek et al., 2005).
(ii) *Available root zone SWC* (θ_{RZ}) calculated from previous time step SWC following depletion by *ET* in current time step;
(iii) *Root water uptake* (*RWU*), which is the ratio of potential transpiration (T_p) to the root length (R_L) multiplied by a dimensionless sink term variable, $\propto_{(h)}$, as a function of the absolute soil water pressure head (Feddes et al., 1978):

$$RWU = \frac{T_p}{R_L} \times \propto_{(h)} \quad (1)$$

where T_p is calculated as an exponential function of *LAI* and ET_0 following Ritchie (1972):

$$T_p = ET_0 \times (1 - e^{-k\ LAI}) \quad (2)$$

- k is a constant representing the fraction of PAR reaching the canopy, which ranges between 0.5 and 0.75. R_L in Eq. (1) and *LAI* in Eq. (2) are both derived from the wheat growth model (see following Section 2.4.3);
- *Excess of water* not infiltrating the soil (h) from HYDRUS^{-1}D was used in the runoff flow model (see following Section 2.4.2);
- *FTSW*, which was calculated as the difference between θ_{RZ} and the soil's wilting point (θ_{WP}) divided by the difference between the soil's field capacity (θ_{FC}) and θ_{WP}:

$$FTSW = \frac{\theta_{RZ} - \theta_{WP}}{\theta_{FC} - \theta_{WP}} \quad (3)$$

Fixed values for θ_{FC} and θ_{WP} were used following Amir and Sinclair (1991a, 1991b) in order to maintain the model with the least number of variables as possible on expense of a possible reduction in the model's spatial sensitivity. HYDRUS^{-1}D was set with an open lower boundary layer.

2.4.2. The two-dimensional spatially distributed surface runoff model

The water excess from the rainfall is computed from HYDRUS^{-1}D for each grid cell and each time step and used as input for a spatially distributed runoff flow model. We used a two-dimensional finite difference numerical solution of the diffusive wave overland flow Saint-Venant equations to simulate flow rate between grid cells using GIS layers (i.e. flow direction, flow accumulation and slope; Julien et al., 1995):

$$q_{(i \to i+x)} \Delta t = \frac{h_i^{5/3}\ s_{(i \to i+x)}^{1/2}}{n_i\ W} \times \Delta t \quad (4)$$

where $q_{(i \to i+x)}$ is the surface runoff flow from grid-cell i to grid-cell $i + x$ and Δt is the timeframe of flow (in minutes; one minute in the runoff model). h_i is the excess water from HYDRUS^{-1}D in grid-cell i and $s_{(i \to i+x)}$ is the slope between the two grid-cells i and $i + x$; while n_i is the Gauckler–Manning coefficient for grid-cell i and W is the grid-cell size (50 m).

At the end of each day of the simulation, the net daily runoff at each designated cell was added to the rainfall input for the first minute of the next day as HYDRUS^{-1}D forcing. This allowed the model to account for grid-based lateral water inputs contributed by neighboring cells (surface runoff flow) in addition to the vertical input from rainfall (derived from the weather radar information).

2.4.3. The Monteith-type wheat growth model

The mechanistic wheat growth model proposed by Amir and Sinclair (1991a, 1991b) was used to simulate AGB and GY. The numerical model of Amir and Sinclair (1991a, 1991b) simulates the following parameters:

(i) *Plant development stages* (leaf out, flowering and grain filling stages) are derived from the physiological time required to reach each stage following a stage-specific thermal unit threshold (Amir and Sinclair, 1991a). Thermal units (TU) are calculated as accumulated Celsius degrees from daily mean temperatures. A physiological time of 103 TU was used for leaf developments, while a maximum of 8 leaves was grown on the main steam and a maximum of 6 on secondary branches (Amir and Sinclair, 1991a). Secondary leaves start to grow when there are already 3 primary leaves on the steam. The physiological time required to reach the second stage, between the end of the leaf out stage to the beginning of the flowering stage is 520 TU for late, 460 TU for moderate and 370 for early developing cultivars. The last grain filling stage lasts for 90 TU and starts when the flowering stage reaches 550 TU.
(ii) *LAI* is calculated from the main-stem leaf area and the number of leaves using an empirical relationship (Amir and Sinclair, 1991b) and an initial density of 240 plants m^{-2}.
(iii) *AGB* is calculated using the radiation use efficiency Monteith's formulation (Monteith, 1977):

$$AGB = APAR \times RUE \quad (5)$$

Where AGB is the aboveground biomass in g m^{-2} and *APAR* is the absorbed PAR (MJ) by the plants; and *RUE* is the radiation use efficiency (g m^{-2} MJ^{-1}). A value of 1.1 g m^{-2} MJ^{-1} was used for maximum potential *RUE*, which was further adjusted for stressful conditions (see following Eq. (8).

APAR in Eq. (5) was calculated using *LAI* as follows (Amir and Sinclair, 1991a):

$$APAR = (1 - e^{-0.5\ LAI}) \times PAR \quad (6)$$

- *End-of-season GY* is derived from AGB by multiplying the AGB by a Harvest Index (*HI*). Daily *HI* of 0.011 d^{-1} (Amir and Sinclair, 1991a, 1991b) was used to calculate the end-of-season GY by multiplying by the end-of-season AGB and the number of growing days.

Leaf development in Eq. (6) is constrained by plant growth response to soil water content dynamics using a *LAI*-adjusted water stress factor (f_{WS_Leaf}):

$$f_{WS\_Leaf} = 2\ /\ (1\ +\ e^{-8\ FTSW}) - 1 \quad (7)$$

where f_{WS_Leaf} ranges between 0 and 1 and is used as a multiplier of the leaf growth (i.e. *LAI*).

Another limitation related to water stress conditions is exerted on the *RUE* in Eq. (5) using a photosynthetic-adjusted water stress factor (f_{WS_Photos}):

$$f_{WS\_Photos} = 2\ /\ (1\ +\ e^{-14\ FTSW}) - 1 \quad (8)$$

The *RUE* in Eq. (5) is thus multiplied by f_{WS_Photos} to simulate photosynthetic inhibition following water stress conditions.

Two additional parameters not included in the original Amir and Sinclair (1991a)'s wheat growth model were included in this study:

(i) *Day of emergence (DE)*, which indicates the exact date of the plant emergence. The *DE* is an important factor in plant development because plant development is highly dependent on meteorological conditions prevailing during the plant emergence stage. We used seeding date information and SWC at a soil-layer depth of 3 cm (from HYDRUS^{-1}D) to derive *DE*. Our criterion for plant emergence

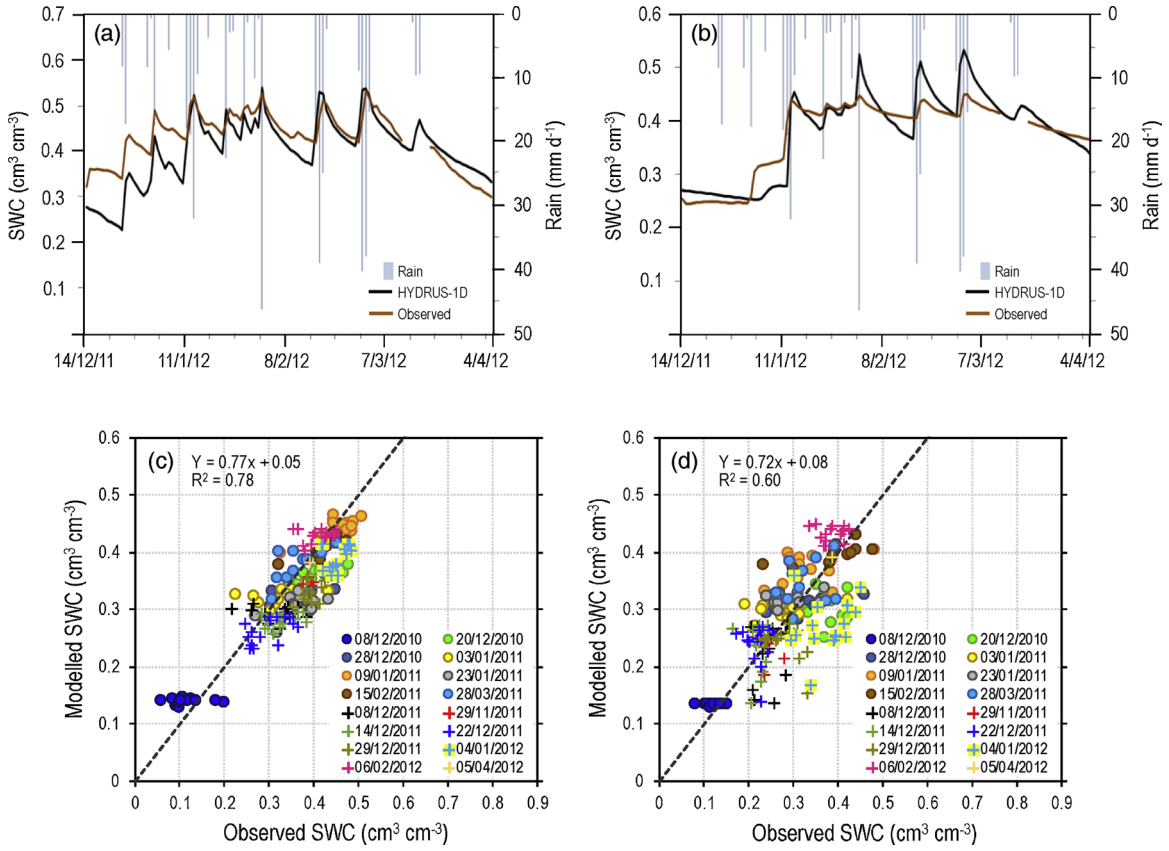

Fig. 3. The 2011/12 seasonal evolution of observed (sensors) and modelled (HYDRUS^{-1}D) volumetric soil water content (SWC) at location A (see Fig. 1c) in the top **(a)** 5–10 cm and a deeper **(b)** 30-cm soil depth. **(c–d)** The baseline comparisons of the gravimetric-derived vs modelled (HYDRUS^{-1}D) SWC per field at soil depths of **(a)** 5–10 cm and **(b)** 30-cm along the season. Colors in **(c)** and **(d)** differentiate between dates. Circles are for 2010/11 season and pluses for 2011/12. Dashed line indicates 1:1 line.

based on previous observations in this region was as follows: when SWC at a 3-cm depth (typical seeding depth) was greater than or equal to θ_{WP} for five consecutive days, then the model was forced to emerge the plant two days later (i.e. at day 7 from seeding). Temperature was not taken into consideration because seedlings rarely experience temperature stress that limits germination in this region.

(ii) *Root length extension* was calculated every day to provide the plant root length/depth in HYDRUS^{-1}D (see section 2.4.1 above). Roots were vertically lengthened by 1 cm each day since the *DE* up to a depth where it reached the wetting front in the soil profile. This allowed us to achieve a more realistic simulation of root water uptake by HYDRUS^{-1}D and an improved simulation of the *FTSW*, because it accounts that way for the changing root zone depth during the growing period.

Finally, the wheat growth model was run on a daily basis (Δ t = 1 d) in dry days and for intervals of 1 min (Δ t = 1 min) in wet days. The runoff model and the one-minute interpolated rainfall data (from the five-minute weather radar data) were used in HYDRUS^{-1}D only for wet days. No local calibration was made to the model in order to keep it as general as possible with a potential application in other areas and under diverse environmental and climatic conditions.

2.5. Model sensitivity analysis

To test the spatial sensitivity of the integrated model at a grid-cell level, we fixed a single input parameter per run with a similar value for all grids and compared our results with observed SWC, AGB and GY. The R^2 value of the simulation was then compared with the R^2 value of the original model (i.e. without fixing the parameter's value). This way, we were able to isolate the effect of the specific parameter, which allowed us to assess its importance in terms of spatial accuracy (i.e. the greater the R^2 of the original model compared to the R^2 of the model with the fixed parameter the greater its importance in the model in simulating spatial variability). Tests were conducted only for dates with a statistically significant spatial correlation between observed and modelled datasets.

Parameters tested were surface runoff, incident radiation load (PAR), rainfall, soil hydraulic parameters, LUM and cultivar (early vs moderate vs late). Rainfall and PAR were fixed with the mean value, while runoff and soil hydraulic parameters were replaced by an average value for all grids (a single mean value for the entire study area for each hydraulic parameter). To test cultivar effect, a single TU value from seeding to flowering was given to all cultivars.

Results are presented as percentage of change in the R^2 of the correlation with respect to the original R^2 using the model without the fixed parameter.

2.6. Evaluation of model performance

We used correlation (R^2), root mean square error (RMSE) and relative RMSE (in %) as measures of the models (HYDRUS^{-1}D and the integrated wheat production model) accuracy. The RMSE and the relative RMSE are defined as:

$$\mathrm{RMSE} = \sqrt{\frac{1}{N}\sum_{i=1}^{N}(Obs_i - Pred_i)^2} \quad (9)$$

$$Relative\ RMSE = 100 \times \frac{RMSE}{Obs_{mean}} \quad (10)$$

3. Results

3.1. Model validation

3.1.1. Hydrus -1D

Fig. 3a,b show the seasonal evolution of observed (sensors) and modelled (HYDRUS^{-1}D) volumetric SWC in the top-soil layers at location A (see Fig. 1c). HYDRUS^{-1}D showed high sensitivity to rainfall, which was in accordance with observed SWC at the shallower soil depth (5–10 cm, Fig. 3a), but less at the deeper 30-cm soil layer (Fig. 3b). The lower sensitivity to rain events of observed SWC at the deeper layer was likely due to low percolation rate, which was less successfully simulated by HYDRUS^{-1}D, as shown in Fig. 3b.

The baseline comparisons of the gravimetric-derived vs modelled SWC (the average SWC using data from all fields and plots) also show a good fit, with R^2 = 0.78 and RMSE = 0.05 cm^3/cm^3 (14%) for the top 5–10 cm soil layer and R^2 = 0.60, RMSE = 0.06 cm^3/cm^3 (22%) for the deeper 30-cm soil layer using data from both seasons (Fig. 3c,d).

Per season correlations were generally better for 2010/11 (R^2 = 0.85 and 0.62 for top 5-10-cm and 30-cm soil depths, respectively) than for 2011/12 (R^2 = 0.73 and 0.45 for top and deeper soil layers) being both high, demonstrating the effectiveness of HYDRUS^{-1}D in simulating accurate soil water dynamics at the plot-level (Fig. 3a,b) and the entire study site (Fig. 3c,d).

3.1.2. The integrated wheat growth model

Fig. 4 shows baseline comparisons of observed vs modelled AGB and GY for both seasons (2010/11 and 2011/12). Modelled AGB and GY from the integrated wheat production model were significantly correlated with observed AGB (R^2 = 0.93; RMSE = 171 g m^{-2}; 31% for both seasons) and GY (R^2 = 0.72; RMSE = 70 g m^{-2}; 13% for both seasons), with relatively low biases of -41 g m^{-2} (8%) and 52 g m^{-2} (10%) for AGB and GY, respectively (Fig. 4).

Per season observed vs modelled AGB correlations were better for 2010/11 than for 2011/12 with R^2 = 0.91 vs 0.73 and RMSE of 216 g m^{-2} (26%) vs 56 g m^{-2} (41%), probably because of the wider range in AGB values in 2010/11 compared to 2011/12 (Fig. 4a). For GY, though, correlations were quite similar for both seasons with R^2 of 0.68 and 0.75 for 2010/11 and 2011/12, respectively (RMSE = 75 g m^{-2} and 59 g m^{-2}; 15% and 11% for 2010/11 and 2011/12, respectively; Fig. 4b).

3.2. Spatial sensitivity test

The spatial sensitivity of the models (HYDRUS^{-1}D and the integrated wheat production model) was tested using observed vs modelled gridded datasets (SWC, AGB and GY) for each date of measurement.

Table 2
Scores of the spatial sensitivity test for **(a)** HYDRUS^{-1}D and **(b)** the integrated wheat production model. R^2 indicates the original score of the model (i.e. the correlation between observed and modelled SWC, AGB and GY without fixing the factor's value). Other scores are percentage of change in R^2 (in % compared to the original model) resulting from the model run with a spatially fixed value for each parameter at a time. Maximum and minimum changes are highlighted in red and blue, respectively. Estimates in **(b)** are AGB collected during the growth season and end-of-season GY. Parameters tested are surface runoff (Q), photosynthetic active radiation (PAR), rainfall (P), soil texture (Soil), land use management (LUM) and cultivar (early vs moderate vs late). The relative change (in %) of the model with fixed values for all parameters is also presented (All).

(a)

SWC	Date	R^2	Q	PAR	P	Soil	LUM	Cultivar	All
5-10 cm	28/12/2010	0.29	10	0	34	34	38	0	55
	09/01/2011	0.51	0	0	0	80	10	0	98
	23/01/2011	0.35	14	3	6	77	0	0	100
	15/02/2011	0.59	0	0	0	95	0	0	98
	14/12/2011	0.31	3	0	0	68	26	0	94
	22/12/2011	0.32	3	0	0	22	6	0	25
	29/12/2011	0.65	2	2	43	60	3	0	62
	04/01/2012	0.70	1	0	90	50	4	0	87
	06/02/2012	0.64	0	0	0	5	2	0	0
30 cm	28/12/2010	0.62	0	0	0	11	13	0	56
	15/02/2011	0.52	0	0	0	71	0	0	88
	AVG	**0.5**	**3**	**0**	**16**	**52**	**9**	**0**	**69**
	min	0.29	0	0	0	5	0	0	0
	max	0.70	14	3	90	95	38	0	100

(b)

Estimate	Date	R^2	Q	PAR	P	Soil	LUM	Cultivar	All
AGB	15/02/2011	0.24	0	8	99	0	0	0	96
	08/05/2011	0.29	3	0	100	21	0	0	72
	06/02/2012	0.85	1	0	24	13	1	0	12
	AVG	**0.46**	**2**	**3**	**74**	**11**	**0**	**0**	**60**
GY	2010-2011	0.55	4	15	54	13	0	0	91
	2011-2012	0.83	1	0	1	17	4	0	61
	AVG	**0.69**	**2**	**7**	**28**	**15**	**2**	**0**	**76**

Sensitivity: Low — High

Table 2 shows results from the model sensitivity tests. Factors that more strongly affected the model's spatial accuracy were colored red, while those having a small or null effect were colored blue.

3.2.1. HYDRUS -1D sensitivity

The factor that mostly affected HYDRUS-1D's spatial accuracy (i.e. the modelled SWC spatial variability) was related to soil hydraulic

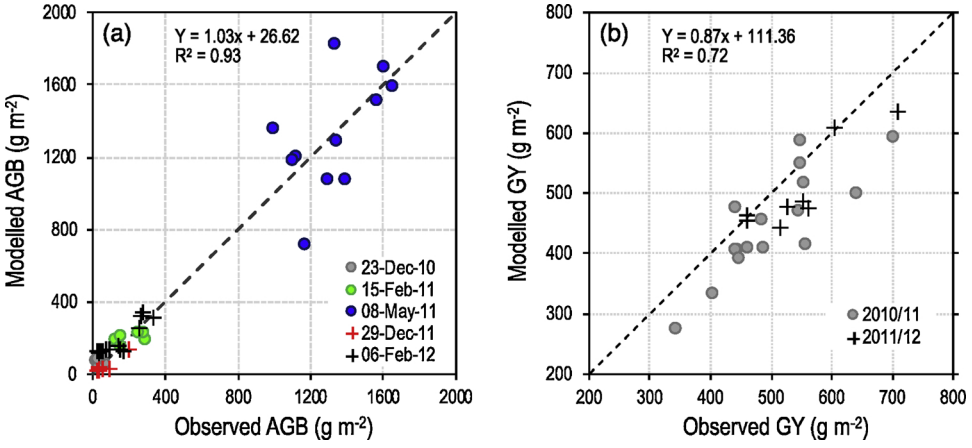

Fig. 4. Observed vs modelled **(a)** aboveground biomass (AGB; g m^{-2}) and **(b)** grain yield (GY; g m^{-2}) per field using data from both seasons (2010/11 and 2011/12). Circles are for 2010/11 and pluses for 2011/12. Colors indicate different dates. Note that end-of-season AGB values for 2011/12 are missing and thus GY values are higher than measured AGB in that season.

parameters (Table 2a). A fixed value for soil texture (i.e. using a single unique value per soil hydraulic parameter for the entire study area) reduced the spatial correlation between observed and modelled SWC by an average of 52% (R^2 was reduced from 0.50 to 0.24, Table S2 in Appendix), with a 5% to 95% range for the examined dates. Rainfall affected HYDRUS-1D spatial accuracy by an average of 19% (range = 0–90%). However, this effect was observed only on SWC at the top-soil (5–10 cm) but not at the deeper 30-cm soil layer. Other parameters affecting HYDRUS-1D spatial accuracy were LUM and, to a lesser extent, surface runoff. Radiation load had only little effect on HYDRUS-1D spatial accuracy while cultivar showed no effect at all (Table 2a).

3.2.2. The wheat production model sensitivity

The spatial accuracy of the integrated wheat production model was mostly affected by rainfall displaying an average spatial accuracy reductions of 74% and 28% for AGB and GY, respectively, when a single fixed rainfall amount was used for the entire study area (Table 2b and Table S3 in *Appendix*). Soil texture (i.e. soil hydraulic parameters) also affected the spatial accuracy of the model but to a lesser extent, with average reductions of 11% and 15% for AGB and GY, respectively. Remaining parameters had only minor impact on the model's spatial accuracy (Table 2b).

3.3. Impacts of temperature and rainfall change on wheat biomass and grain yield productions

The effect of change in temperatures and rainfall amount on AGB and GY were examined with respect to the 2010/11 season.

Fig. 5 shows that temperature and rainfall have both significant but contrasting effects on AGB (Fig. 5a,b) and GY (Fig. 5c,d). Increase in ambient temperatures and decrease in rainfall amount both linearly reduced AGB and GY. According to the model, AGB decreases in average by 150 g m^{-2} (*c.* 10.5% from the 2010/11's AGB) and 110 g m^{-2} (*c.* 7.7%) for 1 °C warming and 5% reduction in rainfall amount, respectively, while GY reductions of 56 g m^{-2} (*c.* 12% from the total GY in 2010/11) and 34 g m^{-2} (*c.* 7.3%) were predicted for similar temperature and rainfall changes.

Fig. 6 shows that AGB and GY reductions following warming and rainfall decrease were not uniformly distributed within the study area. In both simulations, of 1 °C warming and of 5% rainfall reduction, the effect of the north-west to south-east rainfall gradient on the relative reductions of AGB and GY was evident (Fig. 6). Grouping fields by mean annual rainfall amount further corroborated this rainfall gradient effect, with a significant larger change in AGB and GY particularly in the more humid north-west fields (Fig. 7). This rainfall gradient effect was more obvious in the case of GY than in the case of AGB (Fig. 7c,d).

4. Discussion

The integrated model presented in this study links between water infiltration into the soil, water runoff flow and crop growth modeling at a high spatial resolution (50 m). The linkage between surface water dynamics and crop growth is of a great importance, particularly at the start of the season prior to the increase in surface roughness following vegetation growth. The use of three well-established sub-model components allowed to better quantifying water redistribution, which plays an importance role in wheat yield production at semiarid environments (Elliott et al., 2014; Frieler et al., 2017; Helman et al., 2018; Hoffman et al., 2018). Moreover, linking hydrological models with a crop growth model is unique in the sense of the spatially and temporally explicit nature of these models.

All three sub-models, HYDRUS-1D (Simunek et al., 2005), the diffusive wave runoff flow (Julien et al., 1995), and the Monteith-type crop growth model (Amir and Sinclair, 1991b, 1991a), were each successfully used in previous studies. However, here we combined them for the first time to predict wheat biomass and grain yield in a semi-arid environment with great temporal and spatial rainfall variabilities (Goldreich, 1994; Marra and Morin, 2015; Morin and Gabella, 2007).

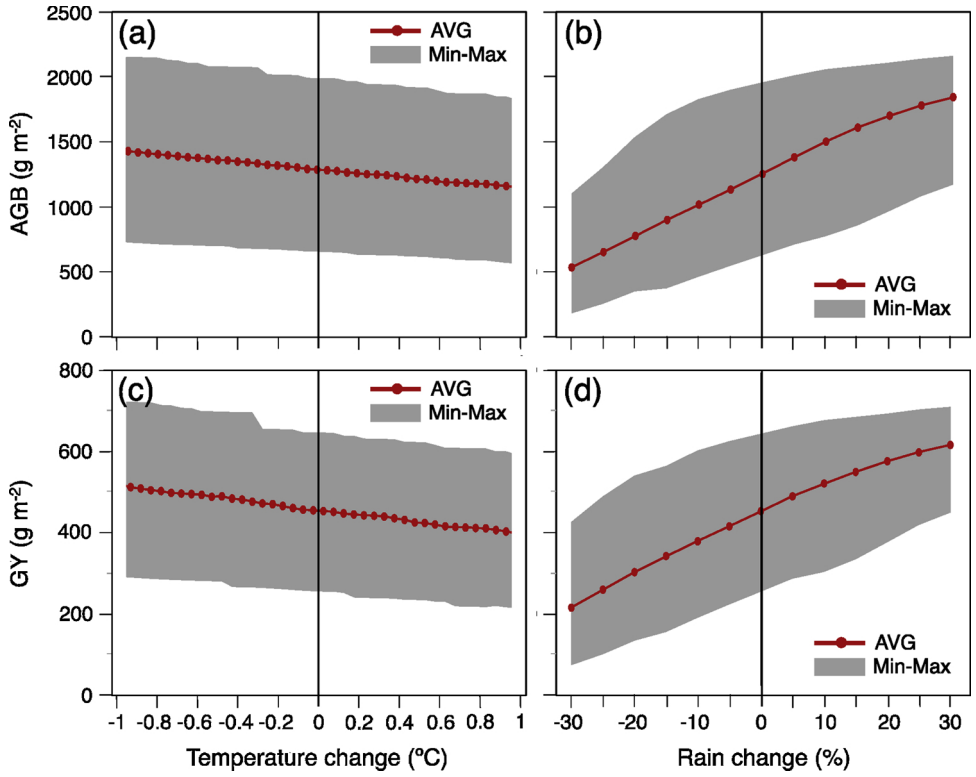

Fig. 5. Predicted changes in **(a–b)** AGB and **(c–d)** GY following changes in **(a,c)** temperature and **(b,d)** rainfall amount. The shaded area indicates the minimum and maximum predicted range of change for the entire study area.

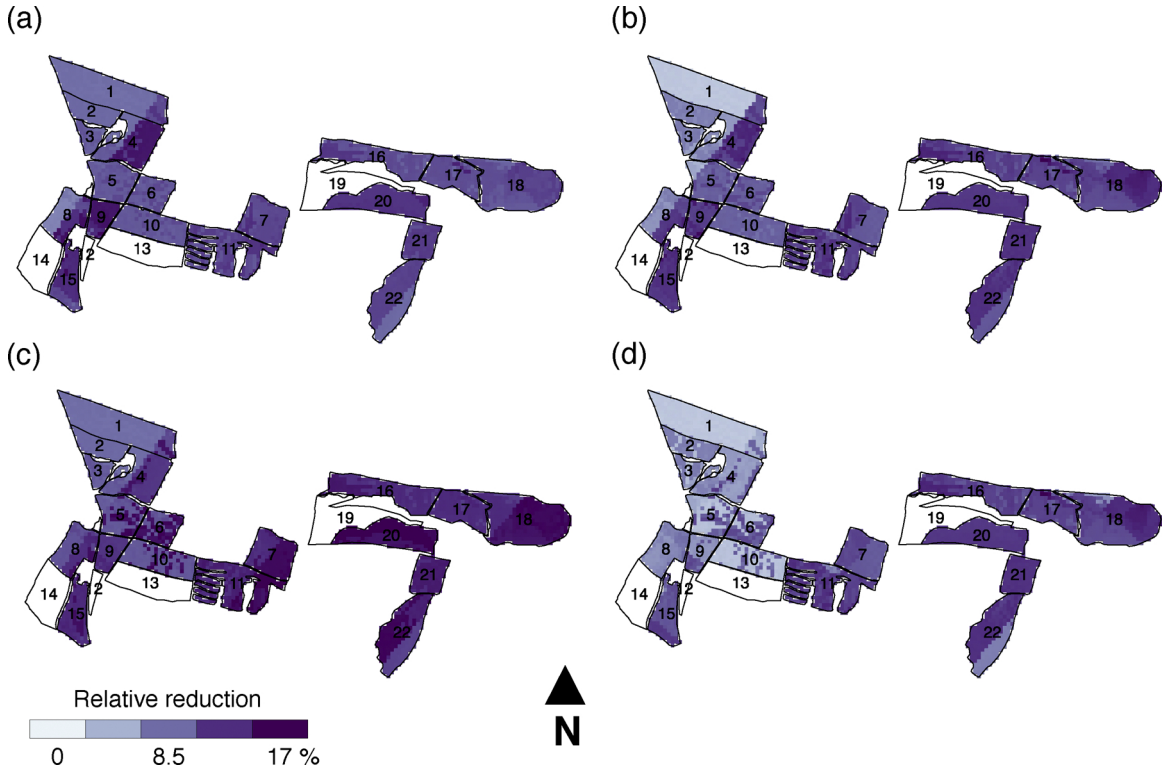

Fig. 6. The spatial distribution of predicted relative (in % compared to 2010/11) reductions without adaptation strategies in **(a–b)** AGB and **(c–d)** GY following **(a,c)** a 1 °C of warming and **(b,d)** a relative reduction of 5% in annual rainfall amount. Note that reductions were not simulated for fields #12, 13, 14 and 19 because wheat was not grown in those fields in 2010/11.

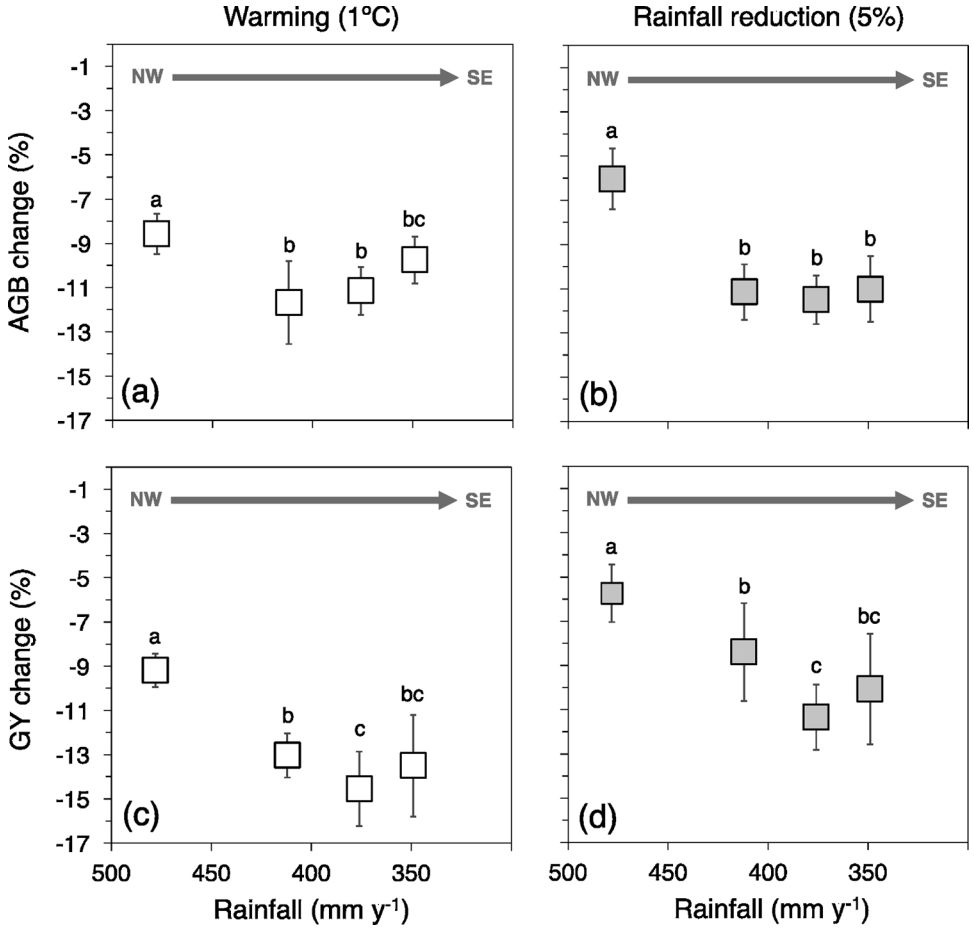

Fig. 7. The effect of the north-west (NW) to south-east (SE) rainfall gradient on **(a–b)** AGB and **(c–d)** GY reductions following **(a,c)** 1 °C warming and **(b,d)** 5% decrease in annual rainfall amount. Changes are relative to AGB and GY productions in 2010/11. Each point in the graphs corresponds to an average value over several fields with a similar mean annual rainfall amount. Error bars are the standard deviation from the average AGB and GY. Different letters indicate statistically significant differences between values.

The use of information such as meteorological radar data allows a more accurate estimation of rainfall spatial variability than using interpolation techniques. Such information is critical for predictions of wheat biomass and grain yield spatial variability because of the vital impact that rainfall variability has on wheat growth in water limited environments (Attia et al., 2016; Saadi et al., 2015).

Mechanistic crop growth models can aid in pre-season and within-season management practices such as in-field fertilizer and irrigation applications (Yin et al., 2017). One of the fundamental goals of growers is to maximize grain yield and net return relative to inputs and production costs through such management decisions (Bonfil et al., 2004; Christy et al., 2018). In that sense, our model has the ability to predict wheat biomass and grain yield changes following weather and environmental changes at the field level assisting growers with management decisions during the growth season, in what is called precision agriculture. By predicting grain yield at the local field scale, growers may better confront possible economic losses due to drought events as well as other environmental disruptions by adjusting their agricultural practices (Bonfil et al., 2004; Guttieri et al., 2001).

Crop growth models have been largely used to investigate wheat growth dynamics over ranges of weather conditions, nitrogen application rates and soil types (Challinor et al., 2009; Chenu et al., 2017; Potgieter et al., 2016). Models may predict, for example, wheat response to applied N in order to improve application recommendations. However, most of the existing crop models require input parameters and information that include extensive weather data, soil parameters, plant characteristics, and crop management factors, which are usually difficult to acquire (Hunt et al., 2001; Jamieson and Semenov, 2000; Sinclair and Amir, 1992). This, often discourages their use in less monitored fields. In other cases, models are applied to a specific field without taking into account spatial variability and effects of neighboring fields (Basso et al., 2012). The integrated model presented in this study requires relatively less input data than other numerical models. It also takes into consideration spatial variability within a field and between fields, which enables forecasting spatial variations in wheat production and yield relatively in an easy manner at the farm level.

Comparisons with SWC sensors showed that HYDRUS-1D was able to capture well water surface dynamics in space and time, which was shown here to be an important factor in predicting spatial variability in wheat growth and yield production (Table 2b). SWC was shown here to be greatly sensitive to rainfall, particularly at the 5–10 cm top-soil layer implying that an accurate input rainfall dataset is required to predict the amount of available water at the root zone. This strengthen the aforementioned claim that rainfall plays a key role in wheat growth processes and that a high-resolution rainfall input data is essential to accurately simulate wheat growth development in rainfed wheat fields (Acevedo et al., 1999; Amir and Sinclair, 1991b).

Meteorological radar systems typically provide rainfall data at resolutions of 100–1000 m in space, and at a temporal resolution of single minutes, which makes them most appropriate for numerical crop growth modelling. However, uncertainties in radar rainfall estimates must be considered prior to its use (Marra and Morin, 2015). At present, only few studies have been used radar rainfall data in wheat production modelling (e.g., Mahtour et al., 2011) and our study calls for more efforts in this direction.

Wheat as a staple food is grown all over the globe and the demand keeps growing. However, wheat production was shown to decrease following warming and may be largely affected by projected warming and water scarcity (Challinor et al., 2016; Deryng et al., 2014; Zhao et al., 2017), particularly in water limited regions (Amir and Sinclair, 1991b; Rajala et al., 2009). To better confront the negative effects of climate change, crop models may assist to improve yield production with proper management actions (Chenu et al., 2017). Using our integrated wheat growth model, we found that warming of 1 °C and rainfall reductions of 5% in the study area might reduce AGB and GY by 10.5% and 12%, and 7.7% and 7.3%, respectively. Such model integration framework may be important to predict yield productions for other areas and/or under different climate scenarios. For example, better management such as changing the sowing date and/or matching the cultivar maturity class to a specific field based on variation in runoff, topographic slope and temperature may be adopted in order to improve yield production in the future. Implementing the proper agricultural practice in the field following simulations from these kinds of models may assist in mitigating reductions in crop yields predicted from climate change.

The proposed model may be initiated with different sowing time, cultivar, supplemental irrigation, etc. to pursue the proper management that farmers should use in their fields. Breeders may test new lines phenology, examining compatibility to new growth condition simulated with our model. In addition, policy makers may use the model to define the required wheat sown area needed to ensure regional food supply (for e.g. by producing similar Figs. 6 and 7 for other areas), as well as to plan grain, hay or silage import or export, according to projected changes in AGB and GY productions.

Although the proposed integrated model does not require local calibration, it should be noted that at least the crop model was developed for the dry conditions typical of the southern part of Israel. This is actually the first time that the crop model is used under more humid conditions in Israel and in soils with different characteristics than those of the southern, dry region of Israel. Nevertheless, the integrated model should be further tested and validated under different climate and environmental conditions to establish its validity in other regions. Moreover, currently the model does not consider carbon and nitrogen sources and thus may be limited to dry regions where water is the dominant factor limiting wheat production and yield.

Finally, our proposed integrated model does not require large computer resources and can be easily run on any standard pc using MATLAB programming language (MathWorks ®). The code for the integrated model is freely available upon request (bonfil@volcani.agri.gov.il). HYDRUS-1D and the runoff model are both commercial software and may be downloaded from the web. Thus, our proposed integrated wheat production model may by easily accessible for use by researchers and wheat growers.

Acknowledgments

David Helman is a Fulbright Fellow 2018/2019. This research was supported by a grant from the Chief Scientist of the Israeli Ministry of Agriculture and Rural Development (IMARD; Grant #857061910). The authors thank Dr Enli Wang and two anonymous reviewers for thorough review and helpful comments, Shacham Mekorot for providing the radar data, the Israel Meteorological Service for the rainfall data and IMARD for sharing the meteorological data. Special thanks to farmers Tal Ofek, Eitan Avivi and Saggy Mark for assistance in collecting samples and data.

References

Acevedo, E.H., Silva, P.C., Silva, H.R., Solar, B.R., 1999. Wheat production in Mediterranean environments. Wheat Ecol. Physiol. Yield Determ. 295–331.

Amir, J., Sinclair, T.R., 1991a. A model of the temperature and solar-radiation effects on spring wheat growth and yield. Field Crop Res. 28, 47–58. https://doi.org/10.1016/0378-4290(91)90073-5.

Amir, J., Sinclair, T.R., 1991b. A model of water limitation on spring wheat growth and yield. Field Crop Res. 28, 59–69. https://doi.org/10.1016/0378-4290(91)90074-6.

Attia, A., Rajan, N., Xue, Q., Nair, S., Ibrahim, A., Hays, D., 2016. Application of DSSAT-CERES-Wheat model to simulate winter wheat response to irrigation management in the Texas High Plains. Agric. Water Manage. 165, 50–60. https://doi.org/10.1016/j.agwat.2015.11.002.

Basso, B., Fiorentino, C., Cammarano, D., Cafiero, G., Dardanelli, J., 2012. Analysis of rainfall distribution on spatial and temporal patterns of wheat yield in Mediterranean environment. Eur. J. Agron. 41, 52–65. https://doi.org/10.1016/j.eja.2012.03.007.

Bonfil, D.J., Karnieli, A., Raz, M., Mufradi, I., Asido, S., Egozi, H., Hoffman, A., Schmilovitch, Z., 2004. Decision support system for improving wheat grain quality in the Mediterranean area of Israel. Field Crop Res. 89, 153–163. https://doi.org/10.1016/j.fcr.2004.01.017.

Boogaard, H.L., Van Diepen, C.A., Rotter, R.P., Cabrera, J., Van Laar, H.H., 1998. WOFOST 7.1; User's Guide for the WOFOST 7.1 Crop Growth Simulation Model and WOFOST Control Center 1.5. SC-DLO.
Brisson, N., Gary, C., Justes, E., Roche, R., Mary, B., Ripoche, D., Zimmer, D., Sierra, J., Bertuzzi, P., Burger, P., Bussière, F., Cabidoche, Y.M., Cellier, P., Debaeke, P., Gaudillère, J.P., Hénault, C., Maraux, F., Seguin, B., Sinoquet, H., 2003. An overview of the crop model stics. Eur. J. Agron. 18, 309–332. https://doi.org/10.1016/S1161-0301(02)00110-7.
Brisson, N., Launay, M., Mary, B., Beaudoin, N., 2009. Conceptual Basis, Formalisations and Parameterization of the STICS Crop Model. Quae.
Cammarano, D., Stefanova, L., Ortiz, B.V., Ramirez-Rodrigues, M., Asseng, S., Misra, V., Wilkerson, G., Basso, B., Jones, J.W., Boote, K.J., DiNapoli, S., 2013. Evaluating the fidelity of downscaled climate data on simulated wheat and maize production in the southeastern US. Reg. Environ. Change 13, 101–110. https://doi.org/10.1007/s10113-013-0410-1.
Cammarano, D., Tian, D., 2018. The effects of projected climate and climate extremes on a winter and summer crop in the southeast USA. Agric. For. Meteorol. 248, 109–118. https://doi.org/10.1016/j.agrformet.2017.09.007.
Challinor, A.J., Ewert, F., Arnold, S., Simelton, E., Fraser, E., 2009. Crops and climate change: progress, trends, and challenges in simulating impacts and informing adaptation. J. Exp. Bot. 60, 2775–2789. https://doi.org/10.1093/jxb/erp062.
Challinor, A.J., Koehler, A.-K., Ramirez-Villegas, J., Whitfield, S., Das, B., 2016. Current warming will reduce yields unless maize breeding and seed systems adapt immediately. Nat. Clim. Change 6, 954–958. https://doi.org/10.1038/nclimate3061.
Chenu, K., Porter, J.R., Martre, P., Basso, B., Chapman, S.C., Ewert, F., Bindi, M., Asseng, S., 2017. Contribution of crop models to adaptation in wheat. Trends Plant Sci. 22, 472–490. https://doi.org/10.1016/j.tplants.2017.02.003.
Christy, B., Tausz-Posch, S., Tausz, M., Richards, R., Rebetzke, G., Condon, A., Mclean, T., Fitzgerald, G., Bourgault, M., O'Leary, G., 2018. Benefits of increasing transpiration efficiency in wheat under elevated CO2 for rainfed regions. Glob. Change Biol. https://doi.org/10.1111/gcb.14052.
Corbeels, M., Chirat, G., Messad, S., Thierfelder, C., 2016. Performance and sensitivity of the DSSAT crop growth model in simulating maize yield under conservation agriculture. Eur. J. Agron. 76, 41–53. https://doi.org/10.1016/j.eja.2016.02.001.
Deryng, D., Conway, D., Ramankutty, N., Price, J., Warren, R., 2014. Global crop yield response to extreme heat stress under multiple climate change futures. Environ. Res. Lett. 9. https://doi.org/10.1088/1748-9326/9/3/034011.
Elliott, J., Deryng, D., Müller, C., Frieler, K., Konzmann, M., Gerten, D., Glotter, M., Flörke, M., Wada, Y., Best, N., Eisner, S., Fekete, B.M., Folberth, C., Foster, I., Gosling, S.N., Haddeland, I., Khabarov, N., Ludwig, F., Masaki, Y., Olin, S., Rosenzweig, C., Ruane, A.C., Satoh, Y., Schmid, E., Stacke, T., Tang, Q., Wisser, D., 2014. Constraints and potentials of future irrigation water availability on agricultural production under climate change. Proc. Natl. Acad. Sci. 111, 3239–3244. https://doi.org/10.1073/pnas.1222474110.
Feddes, R.A., Kowalik, P.J., Zaradny, H., 1978. Simulation of Field Water Use and Crop Yield. Centre for Agricultural Publishing and Documentation, Wageningen.
Fowler, H.J., Blenkinsop, S., Tebaldi, C., 2007. Linking climate change modelling to impacts studies: recent advances in downscaling techniques for hydrological modelling. Int. J. Climatol. 27, 1547–1578. https://doi.org/10.1002/joc.1556.
Frieler, K., Schauberger, B., Arneth, A., Balkovic, J., Chryssanthacopoulos, J., 2017. Understanding the weather - signal in national crop - yield variability. Earth's Futur. 5, 1–12. https://doi.org/10.1002/2016EF000525.
Fu, P., Rich, P.M., 2002. A geometric solar radiation model with applications in agriculture and forestry. Comput. Electron. Agric. 37, 25–35. https://doi.org/10.1016/S0168-1699(02)00115-1.
Gee, G.W., Bauder, J.W., 1979. Particle size analysis by hydrometer: a simplified method for routine textural analysis and a sensitivity test of measurement Parameters1. Soil Sci. Soc. Am. J. 43, 1004–1007. https://doi.org/10.2136/sssaj1979.03615995004300050038x.
Goldreich, Y., 1994. The spatial distribution of annual rainfall in Israel — a review. Theor. Appl. Climatol. 50, 45–59. https://doi.org/10.1007/BF00864902.
Guttieri, M.J., Stark, J.C., O'Brien, K., Souza, E., 2001. Relative sensitivity of spring wheat grain yield and quality parameters to moisture deficit. Crop Sci. 41, 327–335. https://doi.org/10.2135/cropsci2001.412327x.
Hansen, J.W., Jones, J.W., 2000. Scaling-up crop models for climate variability applications. Agric. Syst. 65, 43–72. https://doi.org/10.1016/S0308-521X(00)00025-1.
Helman, D., Lensky, I.M., Bonfil, D.J., 2018. Early prediction of wheat grain yield production from root-zone soil water content at heading using Crop RS-Met. Field Crop Res. (under review).
Helman, D., Bonfil, D.J., Lensky, I.M., 2019. Crop RS-Met: A biophysical evapotranspiration and root-zone soil water content model for crops based on proximal sensing and meteorological data. Agric. Water Manag. 211, 210–219.
Hoffman, A.L., Kemanian, A.R., Forest, C.E., 2018. Analysis of climate signals in the crop yield record of sub-Saharan Africa. Glob. Change Biol. 24, 143–157. https://doi.org/10.1111/gcb.13901.
Holzkämper, A., 2017. Adapting agricultural production systems to climate change—-what's the use of models? Agriculture 7, 86. https://doi.org/10.3390/agriculture7100086.
Huffman, T., Qian, B., De Jong, R., Liu, J., Wang, H., McConkey, B., Brierley, T., Yang, J., 2015. Upscaling modelled crop yields to regional scale: a case study using DSSAT for spring wheat on the Canadian prairies. Can. J. Soil Sci. 95, 49–61. https://doi.org/10.4141/cjss-2014-076.
Hunt, L.A., White, J.W., Hoogenboom, G., 2001. Agronomic data: advances in documentation and protocols for exchange and use. Agric. Syst. 70, 477–492. https://doi.org/10.1016/S0308-521X(01)00056-7.
Jamieson, P.D., Semenov, M.A., 2000. Modelling nitrogen uptake and redistribution in wheat. Field Crop Res. 68, 21–29. https://doi.org/10.1016/S0378-4290(00)00103-9.
Jégo, G., Pattey, E., Morteza Mesbah, S., Liu, J., Duchesne, I., 2015. Impact of the spatial resolution of climatic data and soil physical properties on regional corn yield predictions using the STICS crop model. Int. J. Appl. Earth Obs. Geoinf. 41, 11–22. https://doi.org/10.1016/j.jag.2015.04.013.
Jenson, S.K., Domingue, J.O., 1988. Extracting topographic structure from digital elevation data for geographic information-system analysis. Photogramm. Eng. Remote Sens. 54, 1593–1600.
Julien, P.Y., Saghafian, B., Ogden, F.L., 1995. Raster-based hydrologic modeling of spatially-varied surface runoff. JAWRA J. Am. Water Resour. Assoc. 31, 523–536. https://doi.org/10.1111/j.1752-1688.1995.tb04039.x.
Lawes, R.A., Oliver, Y.M., Robertson, M.J., 2009. Integrating the effects of climate and plant available soil water holding capacity on wheat yield. Field Crop Res. 113, 297–305. https://doi.org/10.1016/j.fcr.2009.06.008.
Liu, J., 2009. A GIS-based tool for modelling large-scale crop-water relations. Environ. Model. Softw. 24, 411–422. https://doi.org/10.1016/j.envsoft.2008.08.004.
Lopez, J.R., Winter, J.M., Elliott, J., Ruane, A.C., Porter, C., Hoogenboom, G., 2017. Integrating growth stage deficit irrigation into a process based crop model. Agric. For. Meteorol. 243, 84–92. https://doi.org/10.1016/j.agrformet.2017.05.001.
Mahtour, A., El Jarroudi, M., Delobbe, L., Hoffmann, L., Maraite, H., Tychon, B., 2011. Site-specific Septoria leaf blotch risk assessment in winter wheat using weather-radar rainfall estimates. Plant Dis. 95, 384–393. https://doi.org/10.1094/PDIS-07-10-0482.
Marra, F., Morin, E., 2015. Use of radar QPE for the derivation of Intensity–Duration–Frequency curves in a range of climatic regimes. J. Hydrol. 531, 427–440. https://doi.org/10.1016/j.jhydrol.2015.08.064.
Monteith, J.L., 1977. Climate and the efficiency of crop production in Britain. Philos. Trans. R. Soc. Lond. B Biol. Sci. 281, 277–294.
Morin, E., Gabella, M., 2007. Radar-based quantitative precipitation estimation over Mediterranean and dry climate regimes. J. Geophys. Res. Atmos. 112. https://doi.org/10.1029/2006JD008206.
Nagaraja Rao, C.R., 1984. Photosynthetically active components of global solar radiation: measurements and model computations. Arch. Meteorol. Geophys. Bioclimatol. Ser. B 34, 353–364. https://doi.org/10.1007/BF02269448.
Palosuo, T., Kersebaum, K.C., Angulo, C., Hlavinka, P., Moriondo, M., Olesen, J.E., Patil, R.H., Ruget, F., Rumbaur, C., Takáč, J., Trnka, M., Bindi, M., Çaldağ, B., Ewert, F., Ferrise, R., Mirschel, W., Şaylan, L., Šiška, B., Rötter, R., 2011. Simulation of winter wheat yield and its variability in different climates of Europe: a comparison of eight crop growth models. Eur. J. Agron. 35, 103–114. https://doi.org/10.1016/j.eja.2011.05.001.
Potgieter, A.B., Lobell, D.B., Hammer, G.L., Jordan, D.R., Davis, P., Brider, J., 2016. Yield trends under varying environmental conditions for sorghum and wheat across Australia. Agric. For. Meteorol. 228–229, 276–285. https://doi.org/10.1016/j.agrformet.2016.07.004.
Rajala, A., Hakala, K., Mäkelä, P., Muurinen, S., Peltonen-Sainio, P., 2009. Spring wheat response to timing of water deficit through sink and grain filling capacity. Field Crop Res. 114, 263–271. https://doi.org/10.1016/j.fcr.2009.08.007.
Ritchie, J.T., 1972. Model for predicting evaporation from a row crop with incomplete cover. Water Resour. Res. 8, 1204–1213. https://doi.org/10.1029/WR008i005p01204.
Rosenzweig, C., Elliott, J., Deryng, D., Ruane, A.C., Müller, C., Arneth, A., Boote, K.J., Folberth, C., Glotter, M., Khabarov, N., Neumann, K., Piontek, F., Pugh, T.A.M., Schmid, E., Stehfest, E., Yang, H., Jones, J.W., 2014. Assessing agricultural risks of climate change in the 21st century in a global gridded crop model intercomparison. Proc. Natl. Acad. Sci. 111, 3268–3273. https://doi.org/10.1073/pnas.1222463110.
Saadi, S., Todorovic, M., Tanasijevic, L., Pereira, L.S., Pizzigalli, C., Lionello, P., 2015. Climate change and Mediterranean agriculture: impacts on winter wheat and tomato crop evapotranspiration, irrigation requirements and yield. Agric. Water Manage 147, 103–115. https://doi.org/10.1016/J.AGWAT.2014.05.008.
Schauberger, B., Archontoulis, S., Arneth, A., Balkovic, J., Ciais, P., Deryng, D., Elliott, J., Folberth, C., Khabarov, N., Müller, C., Pugh, T.A.M., Rolinski, S., Schaphoff, S., Schmid, E., Wang, X., Schlenker, W., Frieler, K., 2017. Consistent negative response of US crops to high temperatures in observations and crop models. Nat. Commun. 8, 13931. https://doi.org/10.1038/ncomms13931.
Simunek, J., Van Genuchten, M.T., Sejna, M., 2005. The HYDRUS-1D software package for simulating the one-dimensional movement of water, heat, and multiple solutes in variably-saturated media. Univ. California-Riverside Res. Reports 3, 1–240.
Sinclair, T.R., Amir, J., 1992. A model to assess nitrogen limitations on the growth and yield of spring wheat. Field Crop Res. 30, 63–78. https://doi.org/10.1016/0378-4290(92)90057-G.
Stöckle, C.O., Donatelli, M., Nelson, R., 2003. CropSyst, a cropping systems simulation model. Eur. J. Agron. 18, 289–307. https://doi.org/10.1016/S1161-0301(02)00109-0.
Stöckle, C.O., Kemanian, A.R., Nelson, R.L., Adam, J.C., Sommer, R., Carlson, B., 2014. CropSyst model evolution: from field to regional to global scales and from research to decision support systems. Environ. Model. Softw. 62, 361–369. https://doi.org/10.1016/j.envsoft.2014.09.006.
Takken, I., Govers, G., Steegen, A., Nachtergaele, J., Guérif, J., 2001. The prediction of runoff flow directions on tilled fields. J. Hydrol. 248, 1–13. https://doi.org/10.1016/S0022-1694(01)00360-2.
Tarboton, D.G., 1997. A new method for the determination of flow directions and upslope areas in grid digital elevation models. Water Resour. Res. 33, 309–319. https://doi.org/10.1029/96WR03137.
Thorp, K.R., DeJonge, K.C., Kaleita, A.L., Batchelor, W.D., Paz, J.O., 2008. Methodology for the use of DSSAT models for precision agriculture decision support. Comput. Electron. Agric. 64, 276–285. https://doi.org/10.1016/j.compag.2008.05.022.

Van Genuchten, M.T., 1980. A closed-form equation for predicting the hydraulic conductivity of unsaturated soils. Soil Sci. Soc. Am. J. 44, 892–898.

Wu, X., Vuichard, N., Ciais, P., Viovy, N., De Noblet-Ducoudré, N., Wang, X., Magliulo, V., Wattenbach, M., Vitale, L., Di Tommasi, P., Moors, E.J., Jans, W., Elbers, J., Ceschia, E., Tallec, T., Bernhofer, C., Grünwald, T., Moureaux, C., Manise, T., Ligne, A., Cellier, P., Loubet, B., Larmanou, E., Ripoche, D., 2016. ORCHIDEE-CROP (v0), a new process-based agro-land surface model: model description and evaluation over Europe. Geosci. Model. Dev. Discuss. 9, 857–873. https://doi.org/10.5194/gmd-9-857-2016.

Yin, X., Kersebaum, K.C., Kollas, C., Manevski, K., Baby, S., Beaudoin, N., Öztürk, I., Gaiser, T., Wu, L., Hoffmann, M., Charfeddine, M., Conradt, T., Constantin, J., Ewert, F., de Cortazar-Atauri, I.G., Giglio, L., Hlavinka, P., Hoffmann, H., Launay, M., Louarn, G., Manderscheid, R., Mary, B., Mirschel, W., Nendel, C., Pacholski, A., Palosuo, T., Ripoche-Wachter, D., Rötter, P., Ruget, R., Sharif, F., Trnka, B., Ventrella, M., Weigel, D., H.-J., E, Olesen, J., 2017. Performance of process-based models for simulation of grain N in crop rotations across Europe. Agric. Syst. 154, 63–77. https://doi.org/10.1016/j.agsy.2017.03.005.

Zhao, C., Liu, B., Piao, S., Wang, X., Lobell, D.B., Huang, Y., Huang, M., Yao, Y., Bassu, S., Ciais, P., Durand, J.-L., Elliott, J., Ewert, F., Janssens, I.A., Li, T., Lin, E., Liu, Q., Martre, P., Müller, C., Peng, S., Peñuelas, J., Ruane, A.C., Wallach, D., Wang, T., Wu, D., Liu, Z., Zhu, Y., Zhu, Z., Asseng, S., 2017. Temperature increase reduces global yields of major crops in four independent estimates. Proc. Natl. Acad. Sci. https://doi.org/10.1073/pnas.1701762114. 201701762.